Progress In Electromagnetics Research Letters, Vol. 27, 33–42, 2011

REALIZATION OF MILLIMETER-WAVE DUAL-MODE FILTERS USING SQUARE HIGH-ORDER MODE CAVITIES

Y. D. Dong[1,*], W. Hong[2], and H. J. Tang[2]

[1]Electrical Engineering Department, 63-129 ENGR-IV, University of California at Los Angeles, Los Angeles, CA 90095, USA

[2]State Key Lab. of Millimeter Waves, School of Information Science and Engineering, Southeast University, Nanjing 210096, China

Abstract—Some interesting results are presented in this paper by investigating the characteristics of square high-order mode cavities. Based on the standard printed circuit board (PCB) process and the substrate integrated waveguide (SIW) technology, two different square cavities which exhibit dual-mode filtering response are studied and implemented. Their bandwidths can be controlled by adjusting the eigen-frequencies of the resonating modes and the coupling apertures. The proposed configurations also allow implementing transmission zeros to improve the selectivity in an easy way. A Q-band quasi-elliptic filter using such two cavities in a folded configuration is designed, fabricated and measured. High selectivity and small insertion loss are achieved which are in good agreement with the simulated results.

1. INTRODUCTION

Recently, the substrate integrated waveguide (SIW), which is synthesized on a planar substrate with linear periodic arrays of metallic vias, has provided a very attractive platform to design low-cost, low-profile, high Q-factor and highly integrated filters [1–11]. Printed circuit board (PCB) is the preferred process for fabricating SIW components due to its low cost and short fabrication cycle compared with LTCC or MEMS process. However, the process restriction and fabrication tolerance limit the application of PCB process for implementing SIW components with reliability at very high frequencies [1, 2]. When the dimension of the resonator is comparable

Received 15 September 2011, Accepted 13 October 2011, Scheduled 18 October 2011

* Corresponding author: Yuan Dan Dong (yddong@ee.ucla.edu).

to the diameter of the metallic vias, the design and fabrication will be extremely difficult, especially for high dielectric materials. In order to implement SIW filters higher than 40 GHz using the normal PCB process, one approach is to enlarge the size of the cavities but using the high-order modes.

Compared with the dominant mode, cavities resonated on high-order modes are able to work at a higher frequency with a larger size. This property can be utilized to design a high frequency SIW filter with PCB process. High-order mode cavities possess a higher unloaded Q value, especially for the circular and square cavities [7], thus smaller insertion loss can be envisioned. Dual-mode resonators are widely used in filter synthesis due to their ability to reduce the number of resonating elements and improve selectivity [7–15]. This paper investigates the characters of the square SIW cavities and presents an alternative scheme to design dual-mode filters with high-order modes. By using two different dual-mode cavities a Q-band filter with a good selectivity, an elliptical filtering response, and low insertion loss is obtained.

2. CHARACTERS OF THE SQUARE DUAL-MODE CAVITIES

Figure 1 depicts the proposed cavity structures designed on the Rogers 5880 substrate with orthogonal input and output feeding lines. Additional metallic posts, or vias, inside the cavity are used to control the resonance frequencies and the propagation of the high-order modes mainly by changing their positions. They are connecting the top surface and the ground. These proposed cavities have a symmetrical configuration in terms of the diagonal line. The coupling scheme and transmission characters of the dual-mode cavities as well as some design consideration are provided in this section.

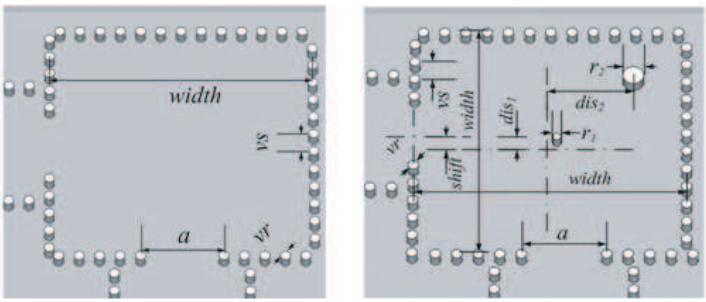

(a) (b)

Figure 1. The proposed dual-mode cavities (a) the first one and (b) the second one with controlling posts inside.

2.1. Coupling Scheme Analysis

Coupling schemes for dual-mode filters have been analyzed according to the particular structures in many papers [7–15]. The filters under this study consist of the classical doublet topology as shown in Fig. 2(a). This structure is known to have a response with one transmission zero if no source to load coupling is considered [13]. The coupling matrix for this doublet is shown in Fig. 2(b). For those high-order modes, self-coupling M_{11} and M_{22} must be considered. It is important to bear in mind that one of the four mutual couplings must be opposite in sign with respect to the sign of the other three couplings which realize the negative coupling [13]. Since the proposed square cavities have a transversal symmetrical configuration in terms of the diagonal line, the values for the coupling from source and load to one particular resonator mode should be the same. For these oversized H-plane cavities we need to look into the phase relation of the magnetic field at the input and output coupling apertures of the cavity to

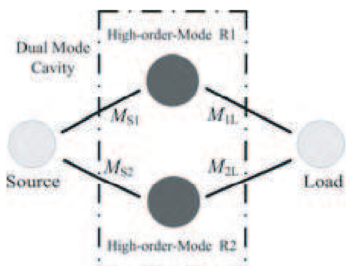

(a)

	Source	R_1	R_2	Load
Source	0	M_{S1}	M_{S2}	0
R_1	M_{S1}	M_{11}	0	M_{1L}
R_2	M_{S2}	0	M_{22}	M_{2L}
Load	0	M_{1L}	M_{2L}	0

(b)

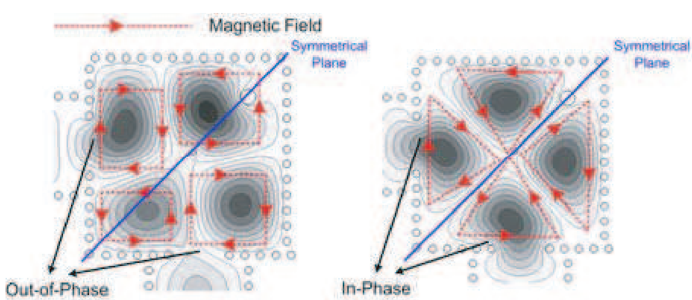

(c)

Figure 2. (a) Coupling scheme and (b) coupling matrix of the proposed dual-mode H-plane cavities, (c) electric and magnetic field of the two resonating modes for the second dual-mode cavity which is used to illustrate the negative coupling.

determine the sign of the coupling coefficient [13, 14]. When the phase undergoes a 180° phase shift between the input and output apertures, we consider that the coupling coefficient has changed the sign which implements the desired negative coupling. One illustrating example is shown in Fig. 2(c) using the second proposed cavity. The resonating modes are two TE_{202}-like modes. The electric and magnetic field distribution is shown in Fig. 2(c). Apparently the input and output couplings for the first mode are out-of-phase while they are in-phase for the second mode. Therefore the first mode generates a negative coupling coefficient with the outside circuits for this dual-mode filter, resulting in one transmission zero. The position of the transmission zero is determined by the relative strength of the two modes [14]. It usually stays close to the weak mode and far away from the strong mode in order to achieve the field balance and the cancelling out.

2.2. Dual-mode Character of the First Square Cavity

The eigen-modes of the square cavity are first investigated. The first degenerate mode is TE_{102} mode. It is shown in [8] and [9] that the TE_{102} mode can also be distributed in the diagonal direction and two TE_{102} modes are suited to a dual-mode filter. The third degenerate mode is TE_{202} mode for which the four lobes are mainly distributed in the four corners and here we call it diagonal-mode as indicated by left plot of Fig. 2(c). The fourth degenerate mode is also TE_{202}-like mode named side-mode for which the lobes are distributed near the border as shown by Fig. 3. The fifth degenerate mode is TM_{020}-like mode as displayed in Fig. 3 and we name it center-mode. From their eigen-frequencies we find that the fourth and the fifth modes are close to each other. By proper arrangement they are expected to realize a dual-mode filtering response. By adopting an orthogonal feeding scheme located in the edge center and a symmetric configuration in terms of the diagonal line, the diagonal mode would not be excited since at the edge center the field is zero for this mode. The simulation shows the feasibility of the idea. Results simulated by HFSS, together with the response obtained directly from the analysis of the coupling matrix are shown in Fig. 3. The values for the matrix are: $R = 1$, $M_{S1} = 0.625$, $M_{S2} = -1.206$, $M_{1L} = 0.625$, $M_{2L} = 1.206$, $M_{11} = -1.68$, $M_{22} = 1.56$. The second mode generates the desired negative coupling. The transmission zero is quite close to the pass-band which leads to a steeper upper side response. In simulation another transmission zero is observed in lower band. However, by analyzing the electric field at that frequency point we find it is caused by the TE_{102} mode and is not in our consideration. Actually this additional transmission zero improves the low frequency stopband rejection.

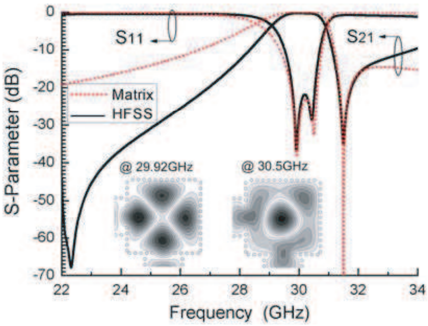

Figure 3. Side-mode and center-mode in the square cavity and the simulated transmission response. The optimized dimensions of the cavity are: $width = 10.4\,\mathrm{mm}$, $vr = 0.4\,\mathrm{mm}$, $vs = 0.8\,\mathrm{mm}$, and $a = 3.29\,\mathrm{mm}$.

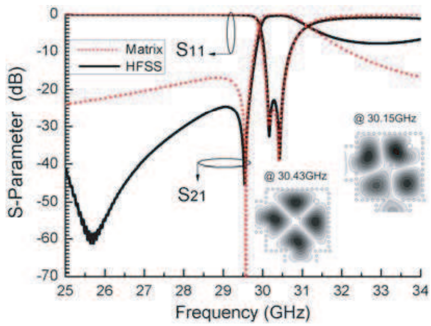

Figure 4. Two different TE_{202} modes and their dual-mode response by coupling matrix and HFSS simulation. The optimized dimensions of the cavity are: $width = 10.2\,\mathrm{mm}$, $vr = 0.4\,\mathrm{mm}$, $vs = 0.8\,\mathrm{mm}$, $a = 3.13\,\mathrm{mm}$, $dis_1 = 0.25\,\mathrm{mm}$, $dis_2 = 3.1\,\mathrm{mm}$, $r_1 = 0.3\,\mathrm{mm}$, $r_2 = 0.8\,\mathrm{mm}$, and $shift = 0.61\,\mathrm{mm}$.

2.3. Dual-mode Character of the Second Square Cavity

As the analysis shown above, although the two different TE_{202} modes (diagonal-mode and side-mode shown in Fig. 4) have a frequency interval with each other, their electric fields are perpendicular just like two TE_{102} modes. Two factors prohibit their dual-mode effect: the resonant frequency and the higher mode (center-mode). In order to solve these problems, first a post is placed in the center of the cavity to suppress the center-mode, which has the strongest electric field in the center. The diagonal-mode and side-mode are nearly not affected by this post because their electric fields are basically the null at the center of the cavity. Secondly, another post is placed in one corner of the cavity as shown in Fig. 1(b). The side-mode is disturbed little by this post; while the diagonal-mode is obviously influenced for its real cavity size is diminished compared to the initial cavity. Then its resonance frequency has been pushed up. The input and output ports are shifted a little in order to provide the required coupling to the diagonal mode but are still orthogonal as shown in Fig. 1(b). Filter performance and optimized dimensions are shown in Fig. 4. The coupling matrix values are: $R = 1$, $M_{S1} = -0.634$, $M_{S2} = 1.123$, $M_{1L} = 0.634$, $M_{2L} = 1.123$, $M_{11} = 1.59$, $M_{22} = -1.46$. The first mode provides the desired negative coupling in this case. An excellent lower band is achieved. The second transmission zero in lower band is also caused by the TE_{102} mode. From the mode pattern it is interesting to note that the four lobes of the two modes keep rotating around the center when the wave is propagating from the input to the output.

2.4. Design Consideration

First the position of the input and output feed lines should be carefully investigated. Generally they should be placed near the strengthened field point of the modes in order to maximize the wave coupling. In above examples they are all right-angled. For the first cavity, feed lines are placed at the center of the two sides, where the electric field of the center-mode and side-mode is strong. Under this scenario the diagonal-mode won't disturb the performance for the output feed-line is at the zero point of its electric field. However for the second cavity the input and output ports are shifted a little from the center in order to couple the wave out for both the side-mode and diagonal-mode.

Transmission zeros are mainly controlled by the position of the input and output feed lines as well as the strength of the particular resonator mode.

The bandwidth of the filters in our study can be easily controlled by adjusting the width of the inductive coupling widows as well as the eigen-mode frequencies. Additional metallic posts can be used for the purpose of bandwidth control. It is more convenient to realize the posts in PCB process than the traditional corner cuts or coupling screws for the rectangular waveguide [12]. In order to obtain a clear understanding, two additional posts are placed near the side center

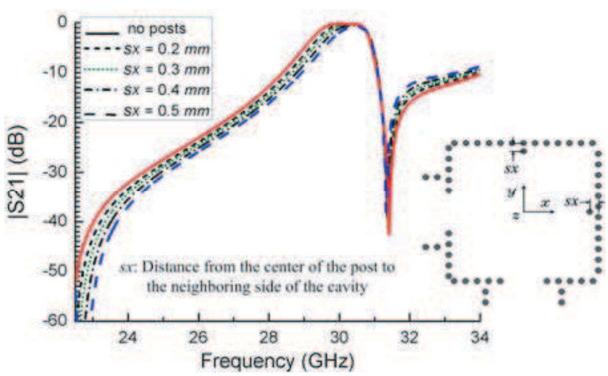

Figure 5. Simulated filter response with different sx for the first cavity.

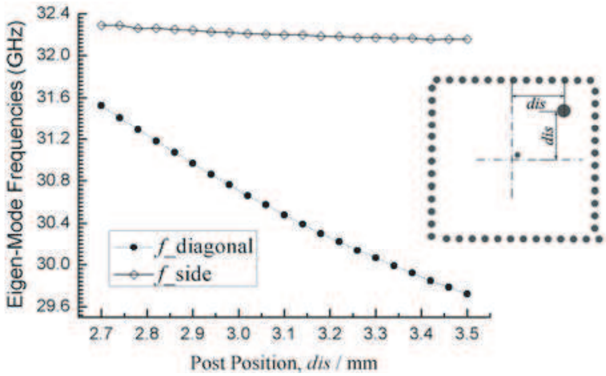

Figure 6. The eigen-mode frequencies for the second cavity with different *dis*.

for the first cavity, which exerts a distinct influence on the side-mode. As shown in Fig. 5, the resonator frequency of side-mode as well as the bandwidth is clearly adjusted by tuning the position of the posts. For the second dual-mode cavity we investigated a square cavity of the same dimension but with a closed structure as indicated by Fig. 6. The relation between the eigen-mode frequencies and the position of the post is presented in Fig. 6. It is seen that the two modes can get quite closer when the post is near the center of the cavity. Note that when the post is very close to the corner or is simply removed, the two modes reach the maximum separation resulting in a wide bandwidth.

3. EXPERIMENTAL VALIDATION

To demonstrate that the proposed cavities work well at even higher frequencies, a Q-band filter (instead of the Ka-band discussed above) which consists of the two cavities shown in Figs. 1(a) and (b) is designed and optimized. The design procedure is the same as the Ka-band filters shown in Figs. 3 and 4. Since the final filter as shown in Fig. 7 is achieved by cascading the two different cavities through an inductive coupling, it preserves all the transmission poles and zeros from the two cavities, which means four poles and two transmission zeros (one transmission zero on each side). This filter is fabricated with PCB process and measured. The substrate used here is Rogers 5880 with a dielectric constant of 2.2 and a thickness of 0.254 mm. Fig. 7 displays the simulated and measured responses of the filter. The filter dimension is shown in the caption of Fig. 7. A photograph of the filter is also shown in the inset of the figure. It is quite compact due to less cavities and a folded configuration. The measured insertion

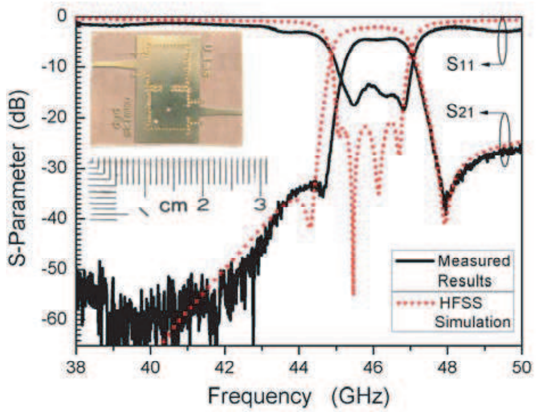

Figure 7. Measured and simulated results of the Q-band two-cavity filter. A photograph of the final fabricated filter is shown in the inset. For the first cavity: $width = 6.79$ mm, $a = 2.32$ mm. For the second cavity: $width = 6.77$ mm, $a = 2.32$ mm, $dis_1 = 0.22$ mm, $dis_2 = 2.32$ mm, $r_1 = 0.3$ mm, $r_2 = 0.6$ mm, and $shift = 0.37$ mm.

loss is about 4.3 dB, which includes the losses of the connectors, 10 mm microstrip and the microstrip-SIW transitions. One similar section of 10 mm microstrip line is also measured for comparison. It is observed that the measured loss of the microstrip line is quite distinct in Q-band, which reaches 1.48 dB at 46 GHz. Thus the real insertion loss for the single filter should be smaller. The measured return loss in pass-band is better than -13 dB. The filter is assumed to be centered at 46 GHz with a 2 GHz bandwidth. Except for the small decrease of bandwidth, the measured results agree well with the simulated results. Small discrepancy should come from the fabrication errors.

4. CONCLUSION

In this study, a novel high-order mode bandpass filter has been investigated and successfully developed at 46 GHz using two square oversized SIW dual-mode cavities. By using additional tuning posts inside the cavity, the bandwidths of the filters can be easily controlled. The filter coupling mechanism has been illustrated in detail. The stopband rejection has been improved by the transmission zeros. This filter is realized using standard PCB process. Low insertion loss, low-profile, good tolerance and high selectivity are achieved. It provides a valuable scheme for the design of high performance filters in millimeter-wave region.

ACKNOWLEDGMENT

This work is supported by National Science Foundation under Grant NSFC60621002.

REFERENCES

1. Tao, Y., W. Hong, and H. J. Tang, "Design of a Ka-band bandpass filter based on high order mode SIW Resonator," *International Conf. on Antennas, Propagation & EM Theory*, 1–3, Guilin, Oct. 26–29, 2006.
2. Chen, X.-P., K. Wu, and D. Drolet, "Substrate integrated waveguide filter with improved stopband performance satellite ground terminal," *IEEE Trans. Microw. Theory Tech.*, Vol. 57, No. 3, 674–683, Mar. 2009.
3. Shen, T. M., C. F. Chen, T. Y. Huang, and R. B. Wu, "Design of vertically stacked waveguide filters in LTCC," *IEEE Trans. Microw. Theory Tech.*, Vol. 55, No. 8, 1771–1779, Aug. 2007.
4. Chen, B.-J., T.-M. Shen, and R.-B. Wu, "Dual-band vertically stacked laminated waveguide filter design in LTCC technology," *IEEE Trans. Microw. Theory Tech.*, Vol. 57, No. 6, 1554–1562, Jun. 2009.
5. Dong, Y., T. Yang, and T. Itoh, "Substrate integrated waveguide loaded by complementary split-ring resonators and its applications to miniaturized waveguide filters," *IEEE Trans. Microw. Theory Tech.*, Vol. 57, No. 9, 2211–2222, Sep. 2009.
6. Lugo, C. and J. Papapolymerou, "Planar realization of a triple-mode bandpass filter using a multilayer configuration," *IEEE Trans. Microw. Theory Tech.*, Vol. 55, No. 2, 296–301, Feb. 2007.
7. Tang, H. J., W. Hong, J. X. Chen, G. Q. Luo, and K. Wu, "Development of millimeter-wave planar diplexers based on complementary characters of dual-mode SIW filters with circular and elliptic cavities," *IEEE Trans. Microw. Theory Tech.*, Vol. 55, No. 4, 776–782, Apr. 2007.
8. Lee, J. H., S. Pinel, J. Laskar, and M. M. Tentzeris, "Design and development of advanced cavity-based dual-mode filters using LTCC Technology for V-band gigabit wireless systems," *IEEE Trans. Microw. Theory Tech.*, Vol. 55, No. 9, 1869–1879, Sep. 2007.
9. Li, R.-Q., X.-H. Tang, and F. Xiao, "An novel substrate integrated waveguide square cavity dual-mode filter," *Journal*

of Electromagnetic Waves and Applications, Vol. 23, No. 17–18, 2523–2529, 2009.

10. Dong, Y. D., W. Hong, H. J. Tang, and K. Wu, "Millimeterwave dual-mode filter using circular high-order mode cavities," *Microwave Opt. Technol. Lett.*, Vol. 51, 1743–1745, 2009.
11. Hu, G., C. Liu, C.-L. Yan, L. Yan, K.-M. Huang, and W. Menzel, "Novel dual mode substrate integrated waveguide band-pass filters," *Journal of Electromagnetic Waves and Applications*, Vol. 24, No. 11–12, 1661–1672, 2010.
12. Liang, X. P., K. Zaki, and A. E. Atia, "Dual mode coupling by square corner cut in resonators and filters," *IEEE Trans. Microw. Theory Tech.*, Vol. 40, No. 12, 2294–2302, Dec. 1992.
13. Soler, F. J., M. M. Mendoza, F. D. Pereira, D. C. Rebenaque, A. A. Melcon, and R. J. Cameron, "Design of bandpass elliptic filters employing inductive windows and dielectric objects," *IEEE Trans. Microw. Theory Tech.*, Vol. 55, No. 11, 2393–2398, Nov. 2007.
14. Amari, S. and U. Rosenberg, "Characteristics of cross (bypass) coupling through higher/lower order modes and their applications in elliptic filter design," *IEEE Trans. Microw. Theory Tech.*, Vol. 53, No. 10, 3135–3141, Oct. 2005.
15. Zhao, L.-P., X. Zhai, B. Wu, T. Su, W. Xue, and C.-H. Liang, "Novel design of dual-mode bandpass filter using rectangle structure," *Progress In Electromagnetics Research B*, Vol. 3, 131–141, 2008.